

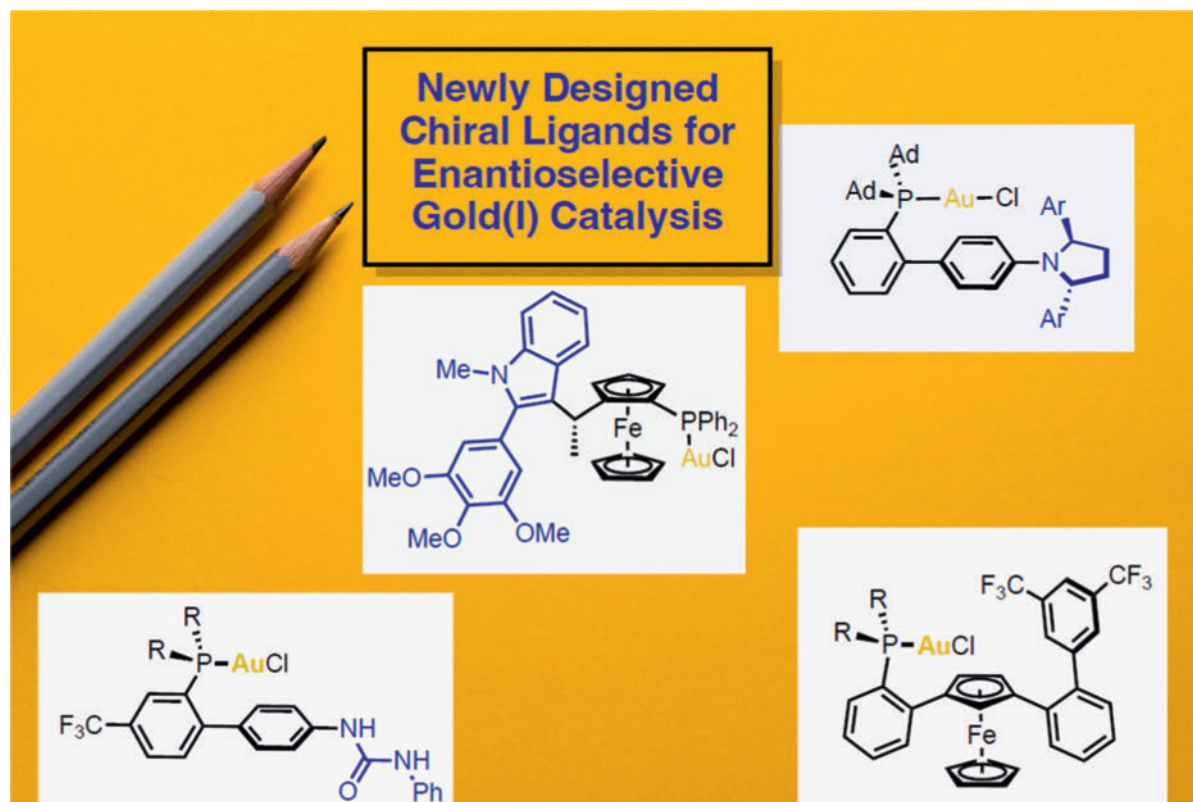
Account

## Tailored-Designed Ligands for Enantioselective Gold(I)-Catalyzed Activation of Alkynes

Pablo Mora<sup>1,2</sup>, Imma Escofet<sup>1</sup>, Antonio Echavarren<sup>1,2</sup>

Affiliation addresses are listed at the end of the article.

### GRAPHICAL ABSTRACT



### ABSTRACT

In this article, we describe the work performed at our laboratories over the years on the design and applications of novel chiral ligands for the enantioselective gold(I)-catalyzed activation of alkynes, with a focus on the cycloisomerization and cycloaddition reactions of 1,6-enynes. The rationale behind the development of each ligand and the mode of enantioinduction are discussed.

**Keywords** Chiral ligands, Enantioselective synthesis, Gold catalysis, Enynes, Alkynes

received May 11, 2025 | accepted after revision July 03, 2025 | article published online August 20, 2025

**Bibliography** Synlett 2025; 36: 3012–3029 DOI 10.1055/a-2650-6278 Art ID ST-2025-05-0210-A

© 2025. The Author(s). Georg Thieme Verlag KG, Oswald-Hesse-Straße 50, 70469 Stuttgart, Germany.

**Correspondence** Prof. Antonio Echavarren, ICIQ, Institute of Chemical Research of Catalonia, Tarragona, Spain, Email: aechavarren@icq.es

## 1 Introduction

Gold(I) complexes are excellent catalysts for the activation of  $\pi$  systems, in particular alkyne-containing substrates. Due to the exquisite alkynophilic character of gold(I) catalysts, the activation of alkynes is highly selective in the presence of other functional groups under very mild conditions.<sup>1</sup> The development of homogeneous gold(I) catalysis initiated with the pioneering work of Teles and Tanaka, who described the selective addition of alcohols and water to alkynes.<sup>2,3</sup> Later, the discovery of the phenol synthesis by Hashmi contributed to the increasing interest and progress of homogeneous gold(I) catalysis.<sup>4</sup> In stark contrast to the impressive progress witnessed in gold(I) catalysis in the last two decades, the development of enantioselective gold(I)-catalyzed transformations evolved at a slower pace. This was mainly a result of the tendency of gold(I) complexes to adopt a bilinear coordination, which places the chiral information provided by ligands far away from the reaction center, resulting in an inefficient enantio-induction. Additionally, the relatively free rotation along the  $L^*-Au$  and the  $Au$ -substrate axis raises the difficulty when fixating the substrate within the chiral environment (Fig. 1). The most common strategies to achieve good enantioselectivities in gold(I) catalysis rely on the use of atropisomeric bisphosphines and phosphoramidites derived from chiral diols such as BINOL and TADDOL, while the use of chiral counterions allows delivering enantioselectivity via tight ion pairing.<sup>5</sup> This latter approach, however, is mainly limited to allenes, as silver phosphates form unreactive phosphine- $Au(I)$  phosphate complexes that are catalytically inefficient in 1, $n$ -enyne cyclizations.<sup>6</sup>

The mentioned strategies have been applied to several enantioselective gold(I)-catalyzed reactions; however, in some cases, the new chiral gold(I) catalysts are only effective for a narrow set of substrates.

Our group explored the use of chiral dinuclear complexes derived from commercially available bisphosphine ligands such as Tol-BINAP or JosiPhos in the alkoxy cyclization of 1,6-enynes and in the intermolecular [2+2] cycloaddition between alkynes and alkenes.<sup>5,7</sup> Due to the limitations discussed above, we decided to develop new chiral ligands customized to overcome

the hurdles dictated by the geometry and particularities of gold(I) catalysis. Similarly, other groups have devoted efforts to implement new and original ligand scaffolds for the enantioselective gold(I)-catalyzed activation of alkynes (Fig. 2).<sup>8</sup>

## 2 Chiral Phosphite Complexes for Cycloisomerization of 1,6-Enynes

Our group described the synthesis of chiral phosphite gold(I) complexes for the enantioselective formal [4+2] cycloaddition of 1,6-arylenynes to form products that have the core structure of the pycnanthuquinone family of natural products (Scheme 1).<sup>9</sup> A screening involving dinuclear bisphosphines, chiral planar, and mononuclear complexes was first conducted, although the enantioselectivities were modest in most cases. A library of gold(I) phosphite complexes was then prepared from enantiopure BINOL using a simple and modular route. Phosphites were preferred over phosphines for their air stability and high reactivity of their gold(I) complexes in the activation of alkynes. Bulky triphenyl silyl groups were placed at the three position of the atropisomeric backbone, while different substituted phenol moieties were explored to introduce the OR group. Phosphite gold complex with a *para*-alkyl substituted phenol **2** led to the highest enantioselectivity (82% ee) in the [4+2] cycloaddition of 1,6-aryl enyne **3**. In combination with  $AgNTf_2$  and performing the reaction  $-20$  °C, it led to the corresponding cycloadduct **4** in 95% yield and 88% ee.

More sterically demanding 1,6-aryl enynes **5–8** were also cyclized, but lower enantioselectivities were obtained. Thus, although our first foray into ligand design for enantioselective gold(I) catalysis was successful, in general, the achieved enantioselectivities were far from optimal.

## 3 Chiral Pyrrolidinyl JohnPhos-Type Ligands

Gold(I) complexes with dialkyl biaryl phosphine ligands have become the catalysts of choice due to their improved reactivity

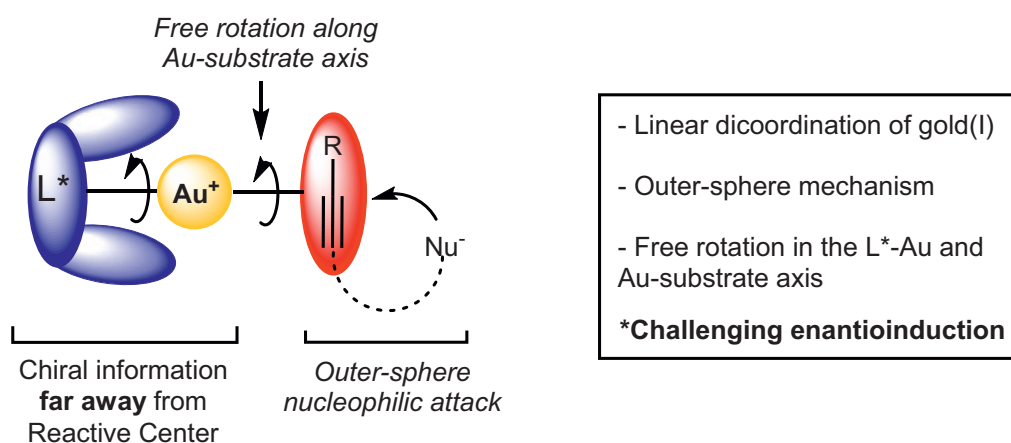
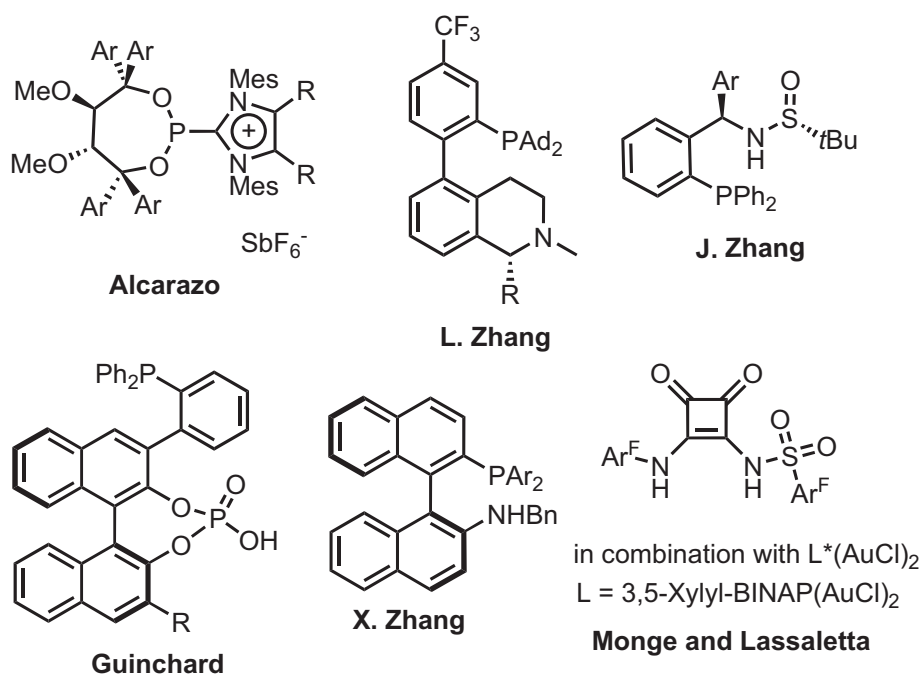
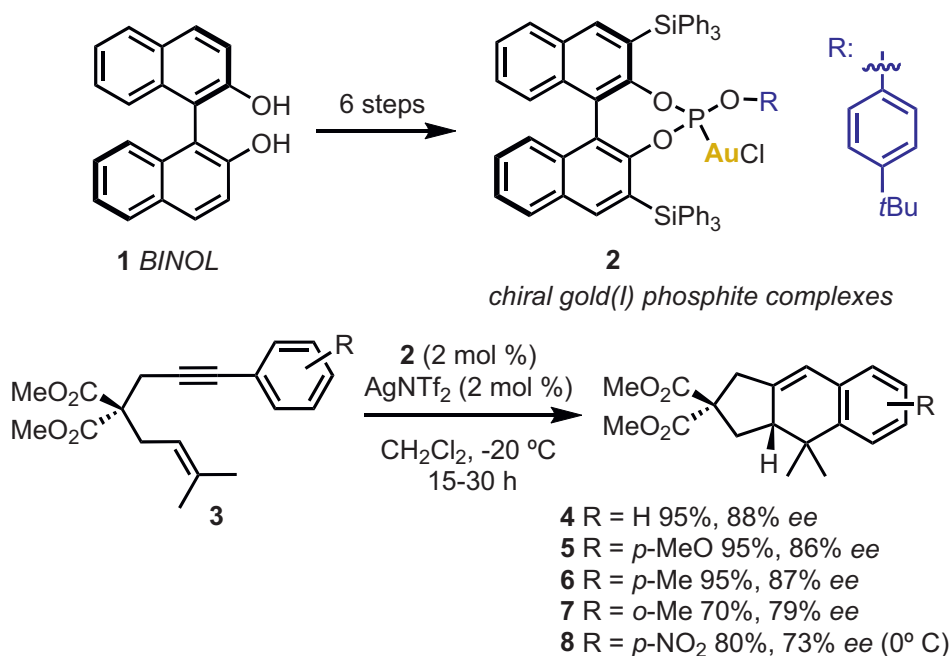


Fig. 1 Challenges associated with enantioselective gold(I) catalysis.



**Fig. 2** Representative ligand scaffolds for asymmetric gold(I) catalysis.

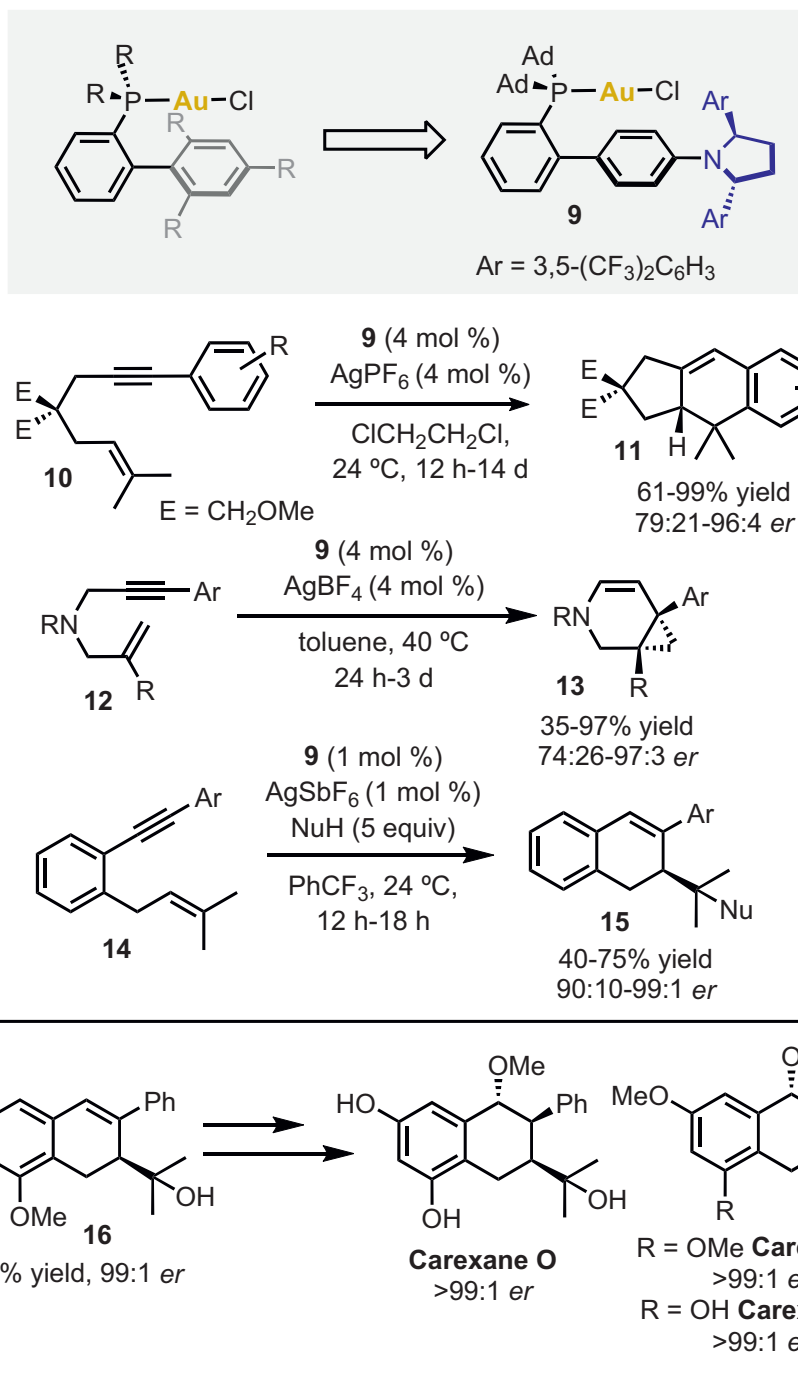


**Scheme 1** Chiral phosphite gold(I) complexes for the enantioselective [4+2] cycloaddition of 1,6-aryl enynes.

across diverse transformations compared to  $PPh_3AuCl$ . Their cationic complexes are easily prepared from the gold chloride precursor using a halide abstractor ( $AgX$  or  $NaB_{Ar}^F$ ) in the presence of a weakly coordinating ligand such as a nitrile (usually MeCN).<sup>10</sup> These cationic complexes are bench-stable and do not require preactivation for catalysis. Hence, we disclosed a new

phosphine ligand featuring a  $C_2$ -symmetric diaryl pyrrolidine at the 4' position of the bottom ring of the JohnPhos scaffold **9** (Scheme 2).<sup>11</sup>

These catalysts allow placing the chiral information next to the reaction center, circumventing the challenges posed by the linear geometry of gold(I). Key to the efficient enantioinduction was the

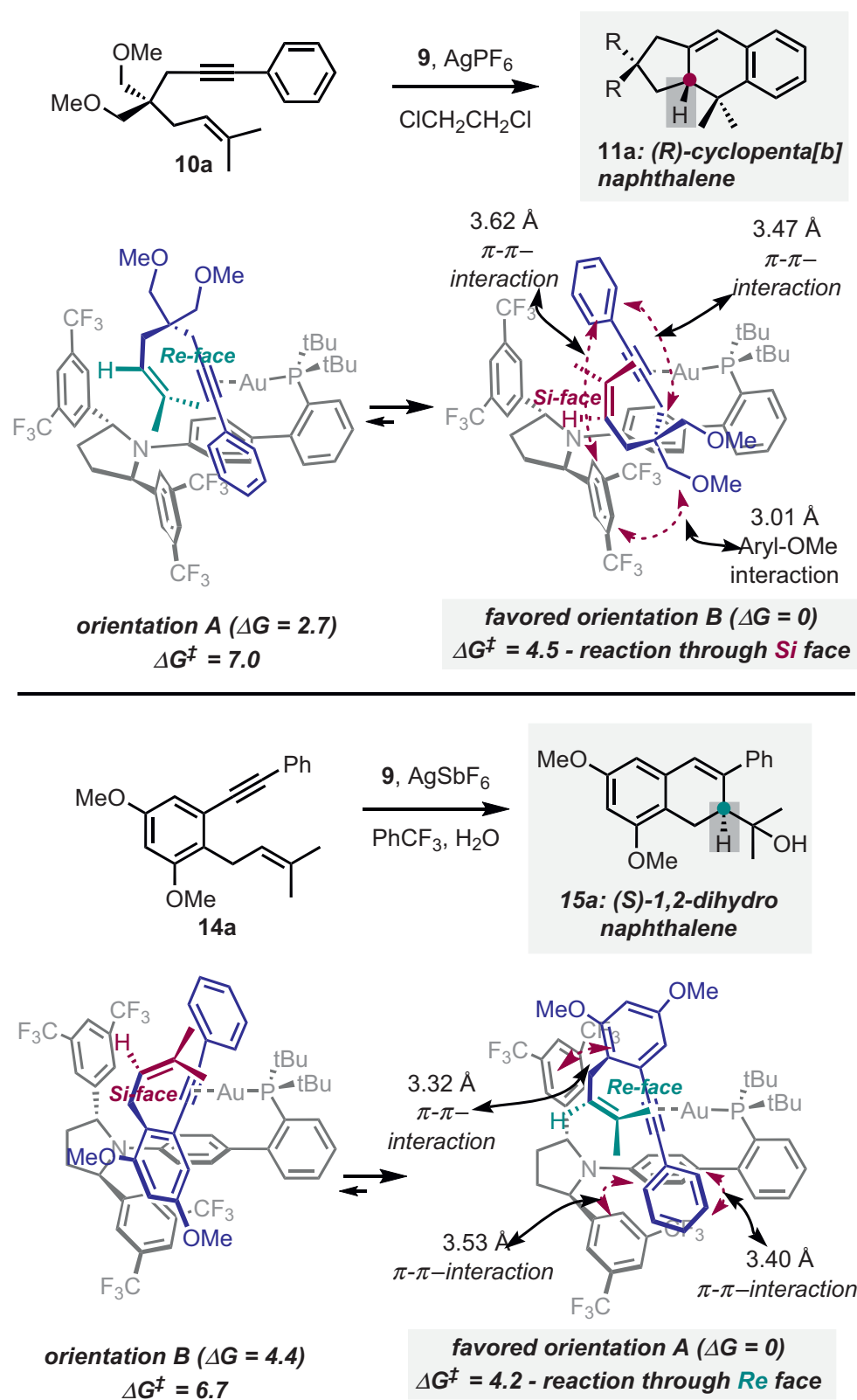


**Scheme 2** Chiral pyrrolidinyl JohnPhos-type ligands for enantioselective folding of 1,6-enynes.

C<sub>2</sub>-symmetric element, which prevents formation of rotamers and the use of a bulky di-adamantly phosphine, which blocks the C–P bond from rotation and forces the P–Au–Cl axis toward the chiral cavity. The new chiral JohnPhos-type gold(I) complexes were applied to three different enantioselective reactions, namely, the formal [4+2] cycloaddition of 1,6-aryl enynes **10**, the cycloisomerization of *N*-tethered 1,6-arylenynes **12** that gives azabicyclo[4.1.0]hept-4-enes **13**, and the (hydro)alkoxycyclization of benzene-tethered 1,6-aryl enynes **14** to afford

1,2-dihydronaphthalenes **15** in good yields and excellent enantioselectivities. Besides, the product of the hydroxycyclization **16** was used in the first enantioselective total synthesis of three members of the carexanes, a family of natural products (**Scheme 2**).

Surprisingly, while these seemingly related cyclizations of 1,6-enynes proceed with good-to-excellent enantiomeric ratios, the first two reactions take place with a facial preference for the *Si* face of the alkene, while the formation of products **15** takes place



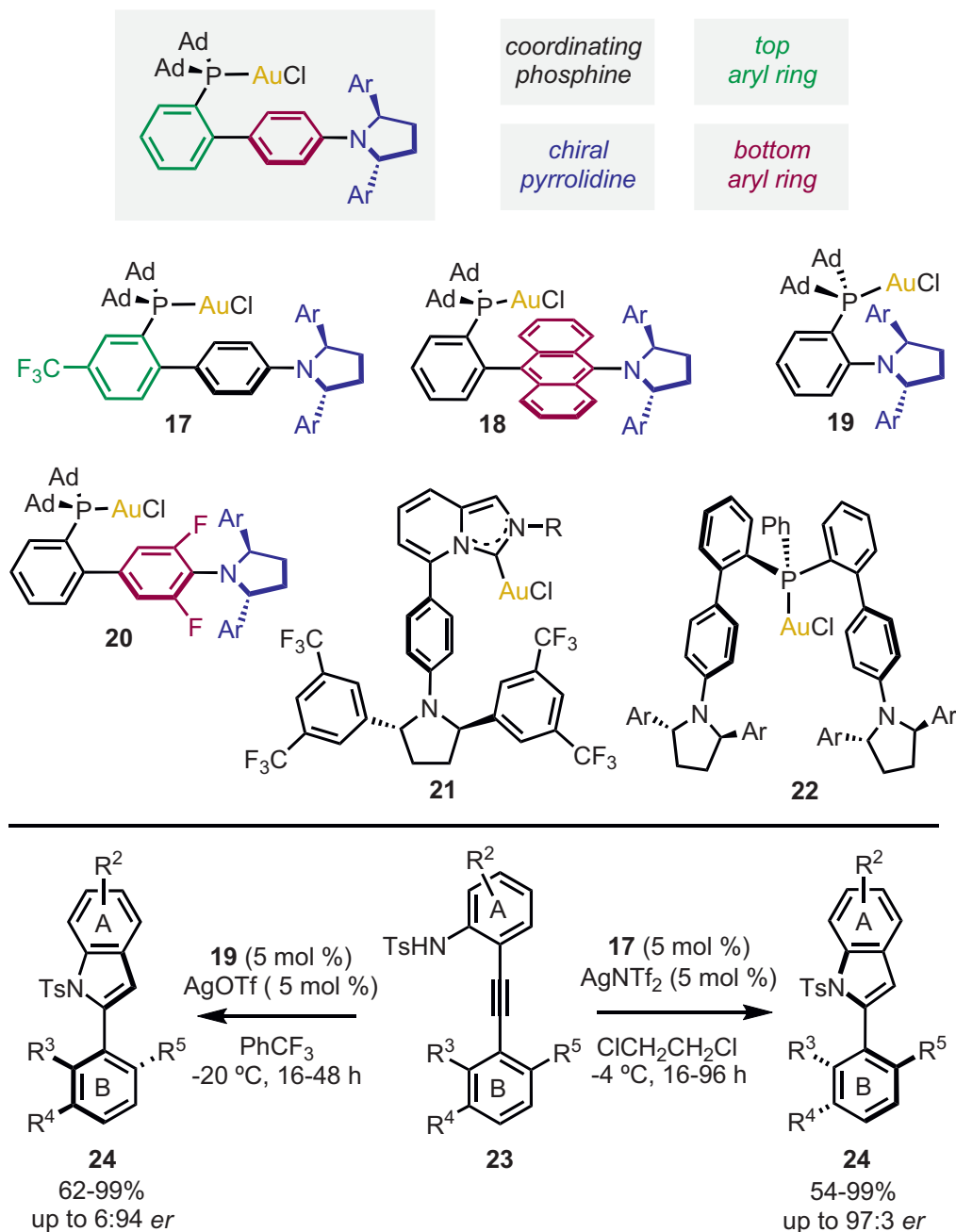
**Scheme 3** Enantioselective folding of enynes **10a** and **14a** and the two-most relevant binding orientations (A and B) with catalyst **9**. Energy values given in kcal/mol relative to the most stable binding orientation in each case.

by reaction of the *Re* prochiral face of the alkene. Computational studies have identified noncovalent attractive  $\pi$ - $\pi$  interactions in the chiral pocket of the catalysts, which are key to achieving good enantioselectivities (Scheme 3). Analysis of the non-covalent interaction (NCI) plots during the folding process revealed attractive interactions between the aromatic moieties of the substrates and those of the chiral diaryl pyrrolidine fragment. The key factor responsible for the enantioselectivity across the three reactions was found to be the  $\pi$ - $\pi$  interactions between the aromatic moieties of the substrates and the remote  $C_2$ -diaryl pyrrolidine,

which induces the specific binding orientation inside the catalyst cavity and stabilizes the transition state.

## 4 Modifications to Chiral Pyrrolidinyl JohnPhos-type Ligands

Based on scaffold **9**, our group prepared a library of gold(I) catalysts featuring a  $C_2$ -symmetric 2,5-diaryl pyrrolidine with several variations including the removal of the bottom ring, enlargement of bottom ring, and the replacement of the phosphine by an



**Scheme 4** Novel variations of the chiral pyrrolidinyl gold(I) complexes and gold(I)-catalyzed atroposelective cyclization toward chiral 2-aryl indoles.

*N*-heterocyclic carbene (NHC) and by diverse bis and tri-aryl phosphine ligands with remote chirality (22 new complexes) (Scheme 4).<sup>12</sup> Other modifications included the introduction of fluorine atoms at the bottom ring, the replacement of aromatic rings in the chiral pyrrolidine for alkyl groups, and the use of *C*<sub>2</sub>-chiral acyclic amines instead of the pyrrolidine.

All the prepared complexes were tested in the intramolecular formal [4+2] cycloaddition of 1,6-aryl enynes **3** and **10** to benchmark their performance and in the atroposelective cyclization of 2-alkynyl sulfonamides **23**, leading to 2-arylindoles **24**.

Placing a CF<sub>3</sub> group at the *meta*-position in the aryl phosphine ring resulted in chiral catalyst **17**, which showed increased reactivity compared to the parent gold complex **9**. Among the second-generation gold(I) catalysts, bulky bis- and tris-biphenylphosphino ligands **22** gave poor enantioselectivities. Likewise, low enantiomeric ratios were determined with complexes **20**-bearing ligands modified at the bottom ring due to reduced flexibility of the chiral diaryl pyrrolidine and ineffective orientation of the chiral cavities. On the other hand, complexes **19**, in which the chiral element is directly attached to the *ortho* position of the phenyl phosphine ring, delivered good enantioselectivities in the [4+2] cycloaddition and the atroposelective cyclization for the formation of 2-aryl indoles. Interestingly, the enantio-divergent formation of 2-arylindoles took place despite the catalysts having the same absolute configuration at the *C*<sub>2</sub>-chiral pyrrolidine.

Recognition of substrate **23a** by catalysts **17** and **19** was evaluated by DFT calculations to identify the importance of the stabilizing NCI (between the sulfonamide and the chiral pocket of catalysts) in determining the preferred reaction pathway. Hence, when using catalyst **17**, intermediate with *R* absolute configuration was preferentially formed through the *proR* face by at least 2.2 kcal/mol, in agreement with the experimental results. Meanwhile, when using the shorter catalyst **19**, the reaction occurred preferentially through the opposite *proS* face, giving rise to the *S* arylindole **24a** (Scheme 5).

The diverse modifications made in the new ligands that were prepared allowed dissecting the most important elements within the ligand scaffold, realizing that subtle changes in the structures of these gold(I) catalysts, such as the introduction of an electron-withdrawing CF<sub>3</sub> group meta to the phosphine phenyl fragment or removal of the bottom ring, have a strong influence, leading to more active and selective catalysts. More abrupt changes, such as enlarging the aromatic bottom ring in complex **18**, were unfortunately detrimental, indicating that those elements close to the chiral pyrrolidine can indeed force ineffective conformations in the catalysts when folding the substrates. In this line, highly bulky bis- and tri-aryl biphenyl complexes were excessively flexible, opening the chiral cavity to accommodate the substrate. Consequently, low enantioselectivities were obtained with these bulky chiral gold(I) complexes. The new family of chiral gold(I) complexes allowed us to identify the most relevant elements in the ligand scaffold bearing a *C*<sub>2</sub>-symmetric diaryl pyrrolidine. Among the catalysts that were synthesized, only gold complexes **17** and **19** showed comparable or better results than complex **9**.

Additionally, a new open-source tool called NEST App was developed to analyze the steric effect in ligands featuring the

cylindrical shape and to predict the enantioselectivities of these complexes (Scheme 6).<sup>12</sup> NEST considers a volume of capsule shape and computes the percent volume occupied by atoms. Dividing the space between the central atom (gold) and the end of the capsule into quadrants, NEST also provides the occupied volumes of the different quadrants that are used as descriptors. Catalysts with experimentally known activity were used to perform single-variable regressions for each descriptor, and the best equation was selected to predict the enantiomeric ratio of systems with unknown reactivity, thereby enabling the development of reliable predictive models. Interestingly, our model was able to predict the stereodivergent formation of products **4a**, **11a**, and **24a**.

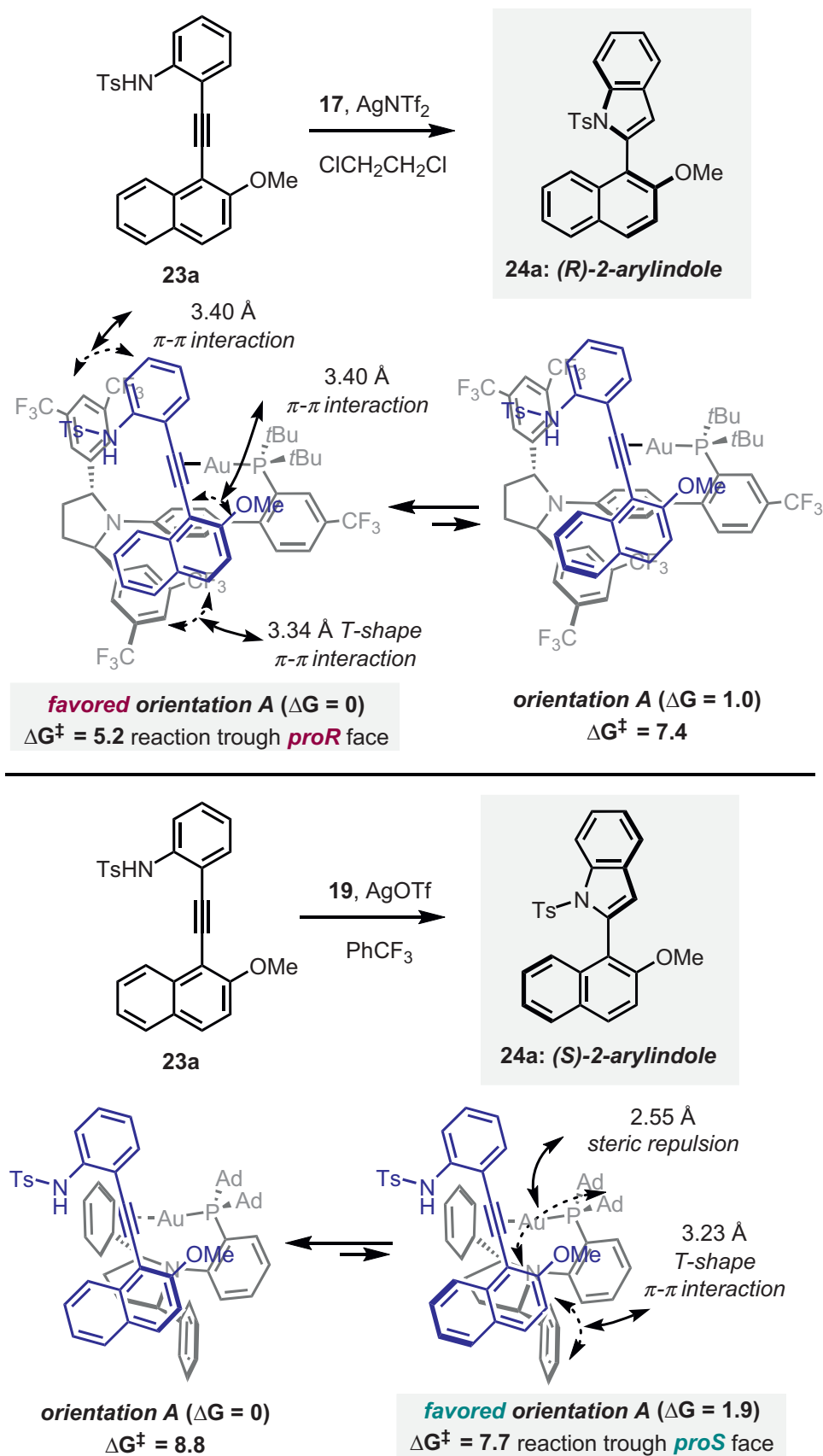
## 5 1,3-Disubstituted Ferrocenyl Gold(I) Complexes

Inspired by the success of chiral pyrrolidinyl JohnPhos-type complexes, we later introduced a family of 1,3-disubstituted ferrocenyl gold(I) complexes **25** in which the chirality is provided by the chiral planarity of the ferrocene scaffold (Scheme 7).<sup>13</sup> These were the first planar chiral analogues of gold(I) catalysts with JohnPhos-type ligands.

In this design, bulky di-adamantyl phosphines were kept in the design to force the Au–Cl axis toward the biphenyl fragment. In a similar fashion to chiral pyrrolidinyl JohnPhos-type gold(I) catalysts, di-substitution at the 3,5-position with CF<sub>3</sub> groups on the top ring of the biphenyl fragment was preferred for higher enantioselectivities. These unprecedented chiral monodentate ligands featured exclusively chiral planarity and allowed performing the [4+2] cycloaddition of 1,6-arylenynes **10** with high enantioselectivity. Computational studies provided a working model showing very good agreement with the experimental results. Analysis of the NCI plots revealed that the biphenyl system engaged in T-shaped π–π interactions with the aryl ring present in the 1,6-aryl enyne. Furthermore, analysis of the steric profile of these ferrocenyl gold(I) complexes showed that the biphenyl substituent provides increased hindrance and higher buried volumes, which are also common in other chiral gold(I) complexes.<sup>14</sup> These novel gold(I) complexes **25** (in total 10 complexes synthesized) showed higher reactivity, allowing the reactions to be conducted at –25 °C using 2 mol% of the chiral catalyst (Scheme 7). However, this family of chiral gold(I) catalysts gave only good enantioselectivities in the formal [4+2] cycloaddition of substrates **10**. In addition, the synthesis of the 1,3-disubstituted ferrocenyl ligands required eight steps from ferrocene.

## 6 1,2-Disubstituted Ferrocenyl Indole Gold(I) Complexes

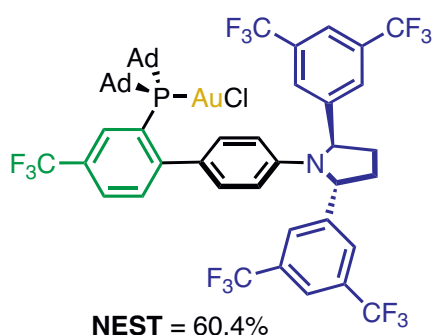
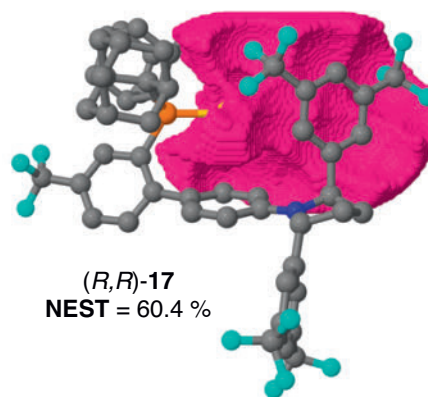
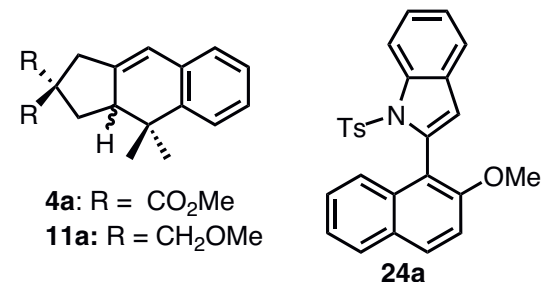
Following up with the previous work using chiral monodentate phosphine ligands and inspired by the work of Hu and Togni on the bidentate ferrocenyl ligand containing heterocycles,<sup>15</sup> we have recently developed a new ligand template based on a 1,2-disubstituted ferrocenyl scaffold (Scheme 8).<sup>16</sup> The ligands were prepared in a convergent manner from commercially available



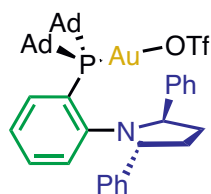
**Scheme 5** Computed pathways for the atroposelective cyclization of **23a** with catalysts **17** and **19** and the two most relevant binding orientations (A and B). Energy values given in kcal/mol are relative to the most stable binding orientation in each case.

## NEST Analysis

- Volume of the complex is a capsule
- Capsule space divided in quadrants
- Provides the % occupied volume
- Building of **predictive models**



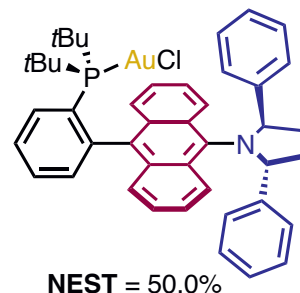
$11a$ : 93:7  $er_{exp}$  – 95:5  $er_{pred}$   
 $24a$ : 88:12  $er_{exp}$  – 82:18  $er_{pred}$



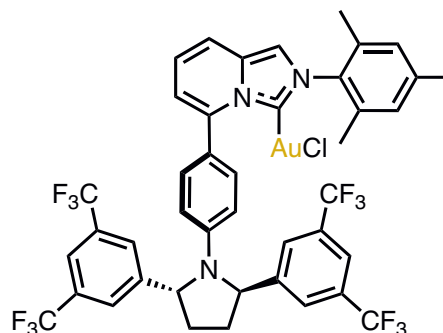
$4a$ : 17:83  $er_{exp}$  – 7:93  $er_{pred}$   
 $11a$ : 15:85  $er_{exp}$  – 20:80  $er_{pred}$   
 $24a$ : 15:85  $er_{exp}$  – 23:77  $er_{pred}$

NEST = 55.0%

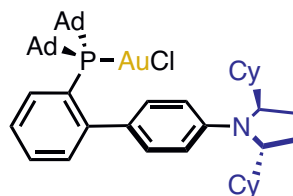
$4a$ : 87:13  $er_{exp}$  – 87:13  $er_{pred}$   
 $11a$ : 70:30  $er_{exp}$  – 80:20  $er_{pred}$   
 $24a$ : 70:30  $er_{exp}$  – 70:30  $er_{pred}$



$11a$ : 44:56  $er_{exp}$  – 50:50  $er_{pred}$   
 $24a$ : 55:45  $er_{exp}$  – 54:46  $er_{pred}$



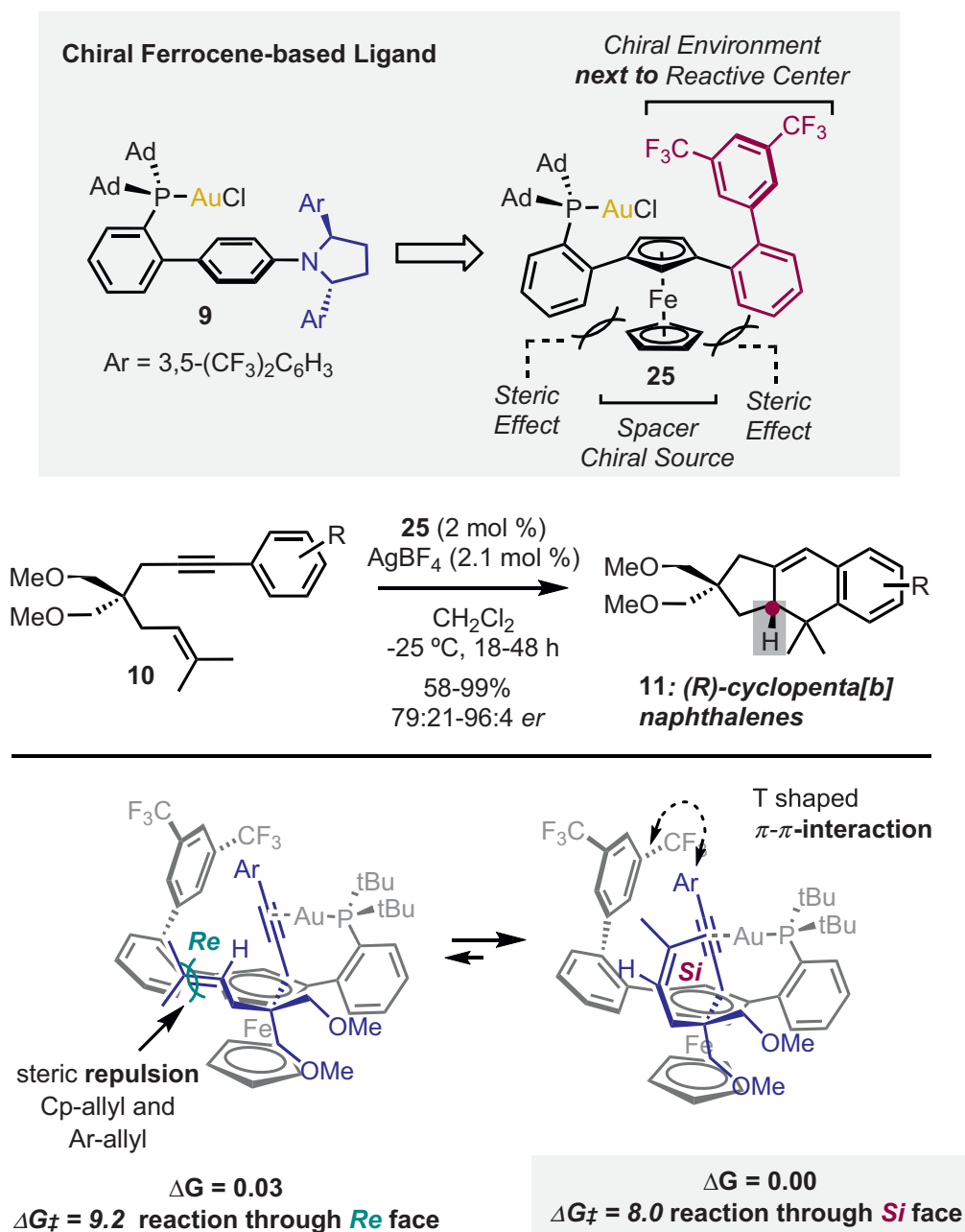
$11a$ : 89:11  $er_{exp}$  – 82:18  $er_{pred}$   
 $24a$ : 67:33  $er_{exp}$  – 74:26  $er_{pred}$



**Scheme 6** NEST Analysis design and occupied volume of selected gold(I) complexes. Selected predicted (pred) and experimental (exp) enantiomeric ratios for the formation of **4a**, **11a**, and **24a**.

enantiopure Ugi's amine and 2-aryl indoles via  $S_N1$  reaction, reducing the synthetic route to four steps. A library of gold(I) complexes (17 examples) was prepared by varying substituents on the 2-aryl indole and the diaryl phosphine, which led to the identification of optimal gold(I) complex **26**.

In contrast to previous designs, an electron-rich arene is preferred in the 2-aryl indole fragment of the gold(I) complex instead of electron-poor aryl rings presented in the 1,3-disubstituted ferrocenyl complex **25** or the chiral pyrrolidiny JohnPhos **9**. A bulky dialkyl phosphine was not necessary, and an

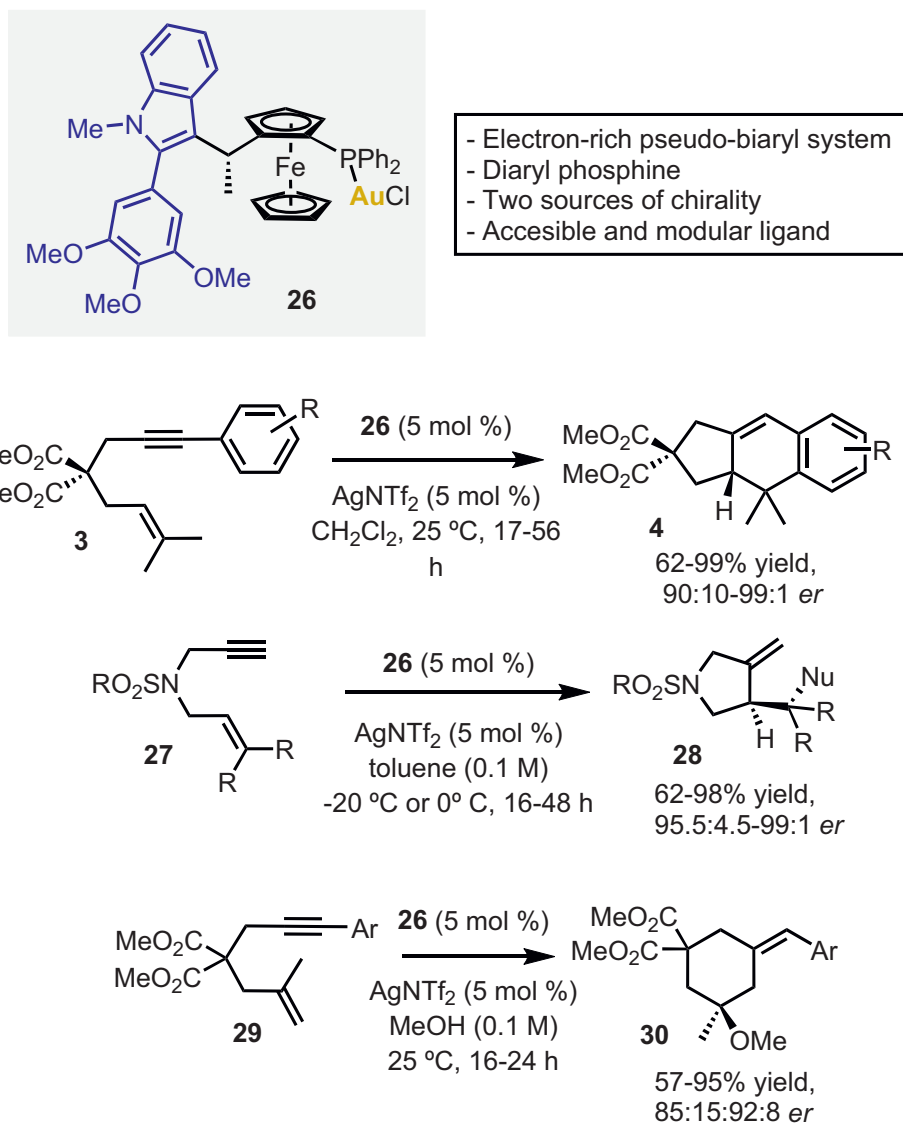


**Scheme 7** New 1,3-disubstituted ferrocenyl phosphines gold complexes and enantioselective [4+2] cycloaddition of 1,6-aryl enynes **10**. Lowest energy transition states of enyne **10** coordinated to catalyst **25**. Energy values are given in kcal/mol relative to the most stable binding orientation in each case.

air-stable diphenyl phosphine gave the best results. The ligand geometry and the benzylic methyl group place the Au–Cl axis toward the chiral cavity. Additionally, NClIs between an axial phenyl phosphine and the indole arm provided robustness to the new chiral ligand. Gold(I) complex **26** gave high enantioselectivity in three gold(I)-catalyzed reactions, namely, the [4+2] cycloaddition of 1,6-arylenynes **3**, the methoxycyclization of 1,6-arylenynes **27**, and the alkoxy cyclization of *N*-tethered 1,6-enynes **29** (Scheme 8). Although previously designed monodentate ligands performed well only with internal alkynes, however, these new chiral

gold(I) catalysts circumvent this limitation by being capable of folding substrates with more challenging terminal alkynes.

The family of gold(I) complexes was evaluated in the [4+2] cycloaddition of 1,6-arylenynes **3** and alkoxy cyclization of *N*-tethered 1,6-enyne **27**. Modes of enantioinduction were unveiled by DFT calculations and analysis of the NCI plots, pointing out that the NClIs between the trimethoxy-substituted aryl ring of the indole of the catalyst and the aryl ring of the substrate are the key elements in the stabilization of the transition state (Scheme 9).

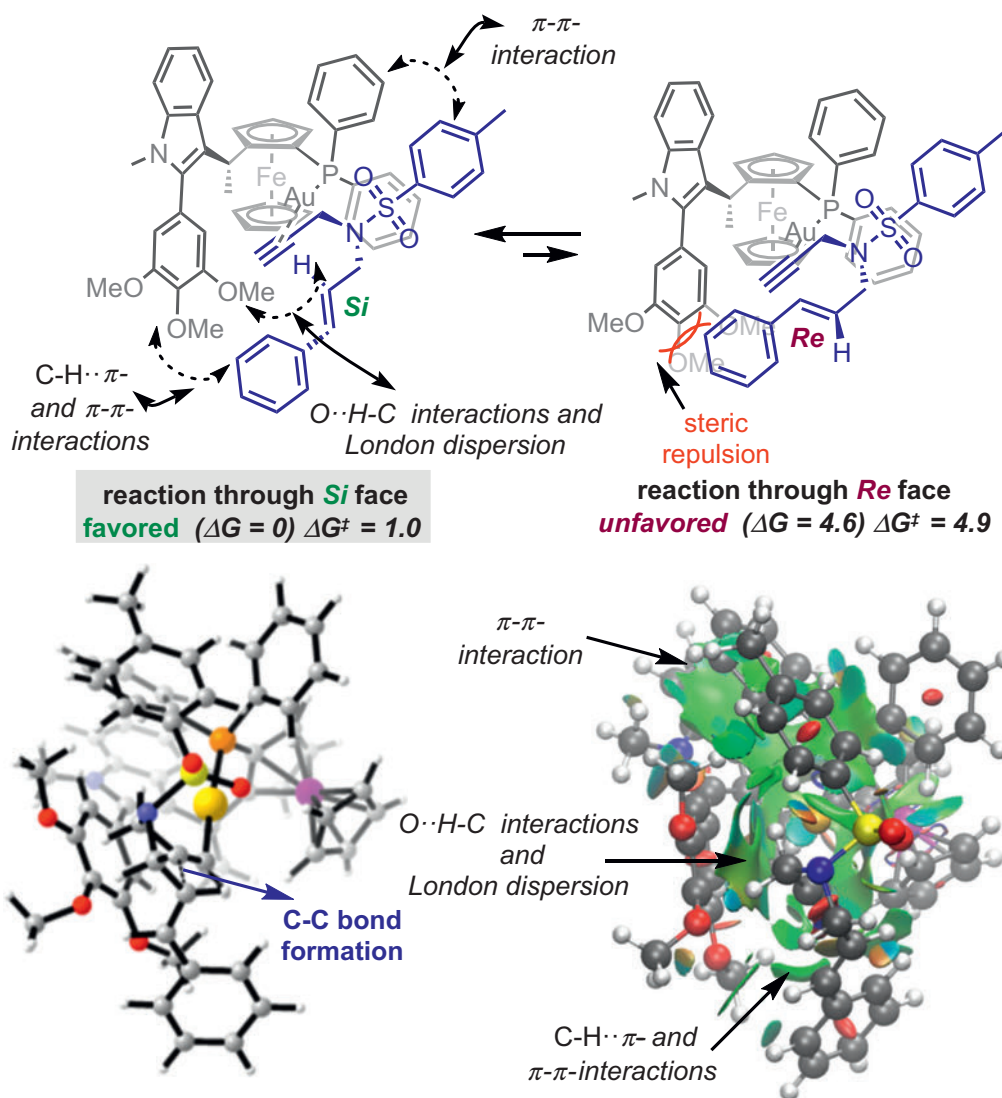


**Scheme 8** Novel 1,2-disubstituted ferrocenyl phosphine gold(I) complexes and their applications in gold(I) catalysis.

The NEST analysis was applied to catalysts of type **26**, which allowed for the reliable prediction of enantioselectivities, highlighting the importance of the size and position of the free space for the substrate coordination and the importance of attractive weak interactions (**Scheme 10**). The experimental data obtained, in combination with DFT-optimized catalyst structures, was used to develop a (multi)linear regression model to predict enantioselectivity. A single descriptor was found to be insufficient, while the combination of two descriptors led to more reliable models to validate and predict enantioselectivities in the two studied reactions. The newly developed NEST analysis and RDKit descriptors turned out to provide good correlation in the predictive models, demonstrating the suitability of this tool when analyzing elongated-shaped chiral catalysts.<sup>11</sup>

## 7 Chiral Resorcin[4]arene Phosphoramidite Ligands

The use of supramolecular systems that mimics the working mode of cyclases to improve the selectivity in metal catalysis has received considerable attention in the last years, with gold(I) cavitands supported by resorcin[4]arenes scaffolds finding use in diverse gold(I)-catalyzed reactions.<sup>17</sup> Based on the resorcin[4]arenes ligands developed by Iwasawa,<sup>17a-c</sup> our group reported chiral gold(I) complexes such as **31** (**Scheme 11**).<sup>18</sup> Chirality was introduced in the phosphoramidite binding site of the cavitand from commercially available chiral bis-(1-arylethyl)amines. Replacing the quinoxaline walls for 1,4-naphthoquinones was explored as well as the formation of mono and dinuclear gold(I) cavitands, leading to a library of chiral gold(I) complexes. These



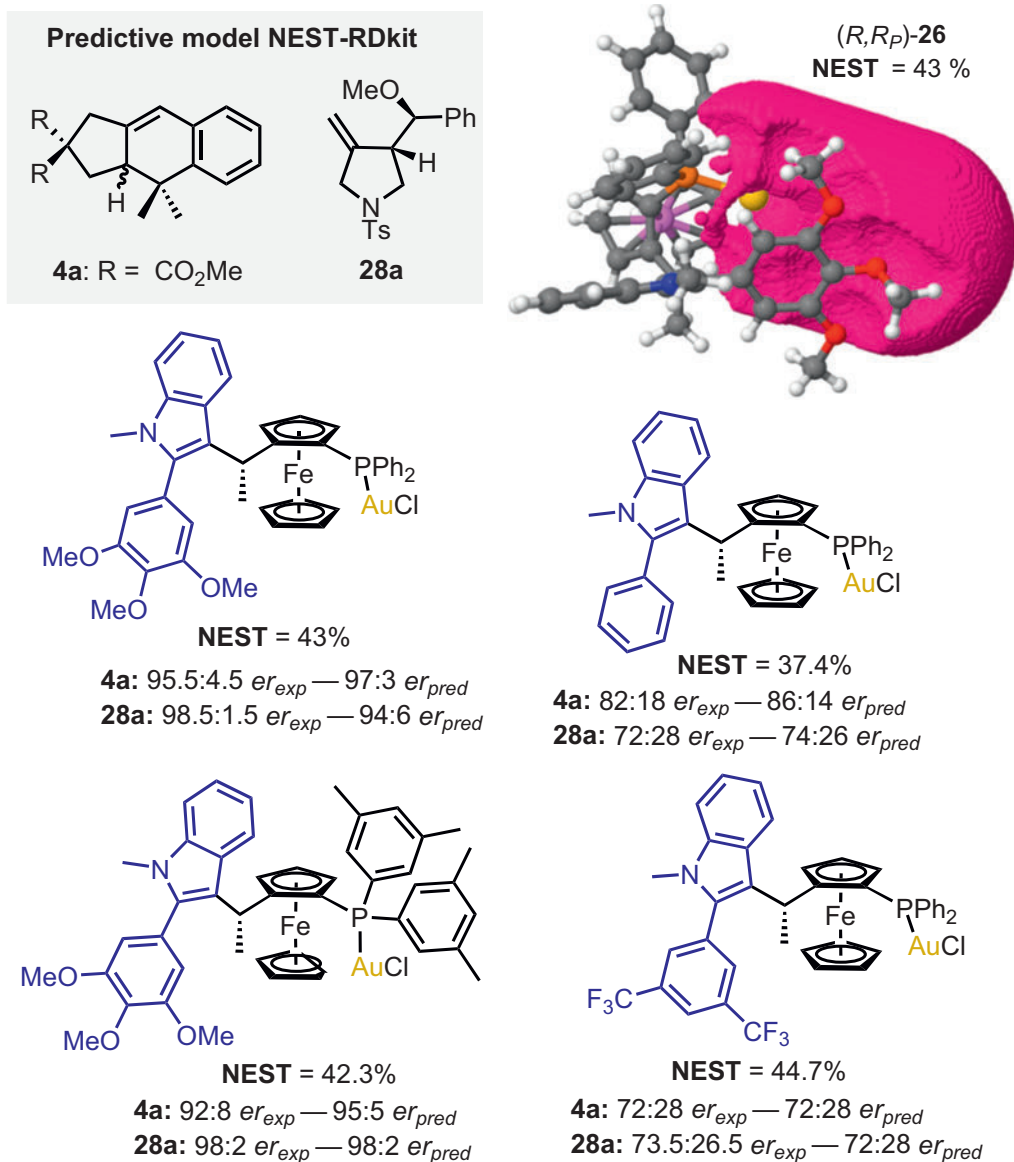
**Scheme 9** Lowest energy intermediates and molecular structures and NCI plots of the transition states for the alkoxy cyclization of *N*-tethered 1,6-enynes **27** with catalyst **26**. Energy values are given in kcal/mol relative to the most stable binding orientation in each case.

chiral gold(I) catalysts were applied in the alkoxy cyclization of benzene-tethered 1,6-enynes **32**. While mononuclear gold(I) complexes gave low enantioselectivities, monocationic dinuclear cavitand **31** delivered the alkoxy cyclization product **33** with high levels of enantioselectivity.

Different enynes and nucleophiles could be cyclized, leading to chiral 2,3-dihydro-1*H*-indene products **33** in excellent enantioselectivities.<sup>18</sup> The enantioselective alkoxy cyclization with chiral gold(I) cavitands was applied in the first total synthesis of the carbazole alkaloid (+)-mafaicheenamine. The effects induced by the cavity and the presence of a non-activated secondary gold(I) center were found to be essential to achieve enantioinduction. NCI plot studies showed that attractive interactions between the cavitand and the aromatic ring of the enyne took place. Additionally, NCIs were observed within the gold complex during the transition state.

## 8 Hydrogen-bonded Counterion-directed Enantioselective Catalysis

Our group developed a new strategy for enantioselective gold(I) catalysis by combining metal catalysis, H-bond organocatalysis, and counterion-directed catalysis (**Scheme 12**).<sup>19</sup> A cationic gold(I) complex containing a H-bond donor in its structure is bound to a chiral BINOL-based phosphoramidite anion via hydrogen bonding, thus creating a chiral supramolecular system **36** for the folding of unsaturated substrates that are held together by NCIs (**Scheme 12**). The new strategy introduced for the first time the use of chiral anions for the gold(I)-catalyzed activation of alkyne substrates. Our group had previously shown that mixing phosphine gold(I) complexes with BINOL-derived phosphates leads to the formation of neutral gold(I) complexes bearing an anionic phosphate ligand, which are not catalytically active.<sup>6</sup>

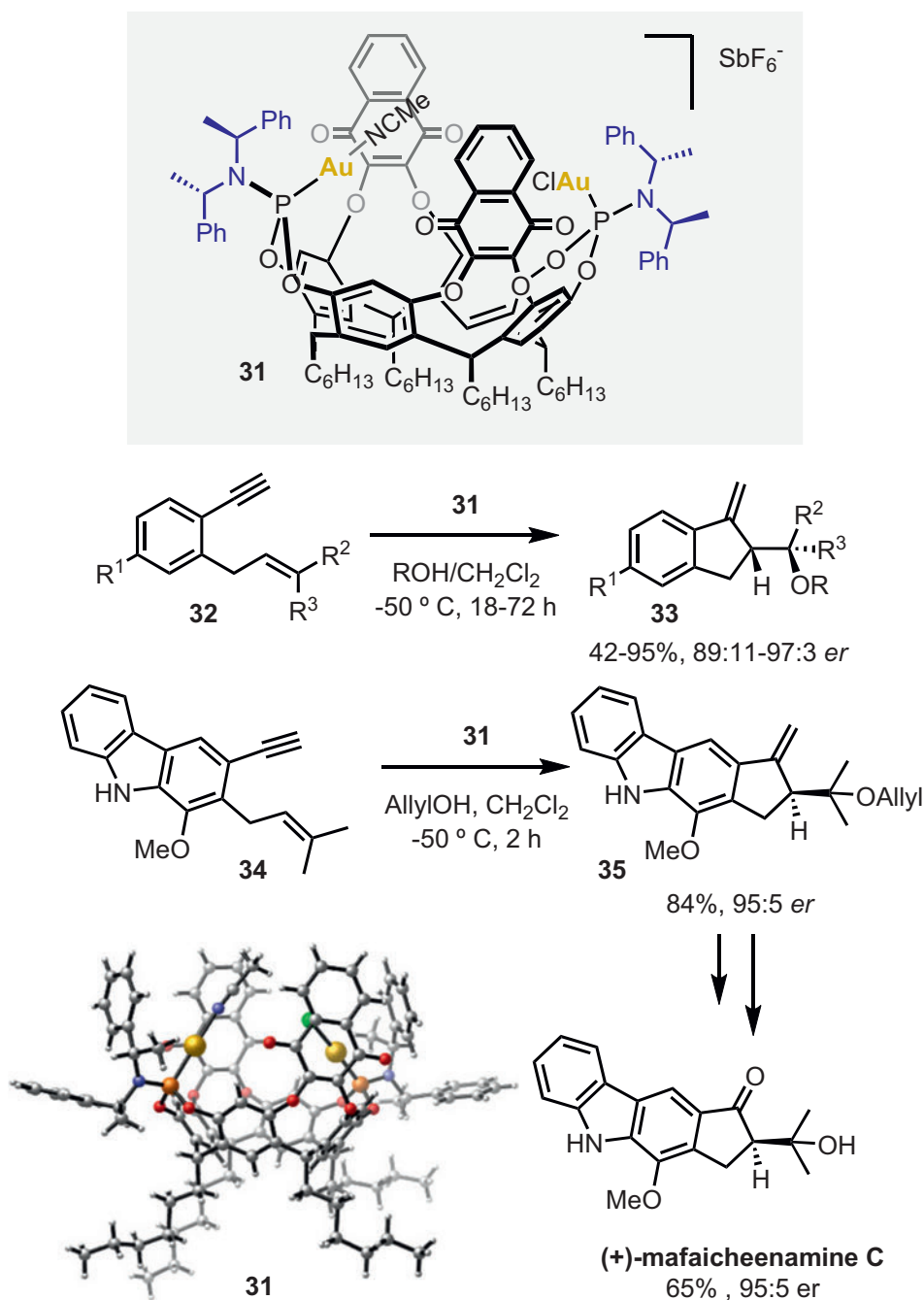


**Scheme 10** NEST analysis, design, and occupied volume of selected gold(I) complexes. Selected predicted (pred) and experimental (exp) enantiomeric ratios for the formation of **4a** and **28a** for each catalyst.

A JohnPhos-type phosphine was selected to support the gold(I) center, and the *meta*- and *para*-positions of the distal ring were functionalized with(thio)ureas and squaramides as “anchor” for the chiral anion. The H-bond donor was envisioned to perform two roles: abstract the halide from the P–Au–Cl, thus allowing substrate coordination, and to anchor the chiral anion close to the substrate to deliver the stereochemical information during the folding process.

The use of a two-component catalytic system was as well advantageous because of the flexibility to quickly tune these two components via high-throughput screening methods. The H-bonded asymmetric-counteranion directed catalysis (ACDC) approach was first validated in the cycloisomerization of 1,6-arylenynes **10**, a well-established gold(I)-catalyzed reaction to benchmark enantioinduction. Different silver salts were tested in

combination with phosphinorea gold(I) complexes, resulting in the identification of *N*-triflyl phosphoramidate salts as the best performer in terms of reactivity and enantioselectivity and **37** as the optimal phosphino urea gold(I) complex (**Scheme 12**). The enantioselectivities obtained were also highly dependent on the substitution at the 3,3'-position of the BINOL skeleton, whereas substitution at phosphorus regulated the coordinating ability and reactivity. After solvent evaluation and fine-tuning of the catalytic system, the substrate scope of the formal [4+2] cycloaddition of 1,6-enynes was explored using **37** and **38**, which delivered the highest yield and enantioselectivities. 1,6-Enynes with different tethers and substitutions were cyclized to give the tricyclic products **11** with high enantioselectivities and yields, demonstrating a broad scope across the substrate set. Furthermore, the standard [4+2] cycloaddition reaction with enynes **10** could



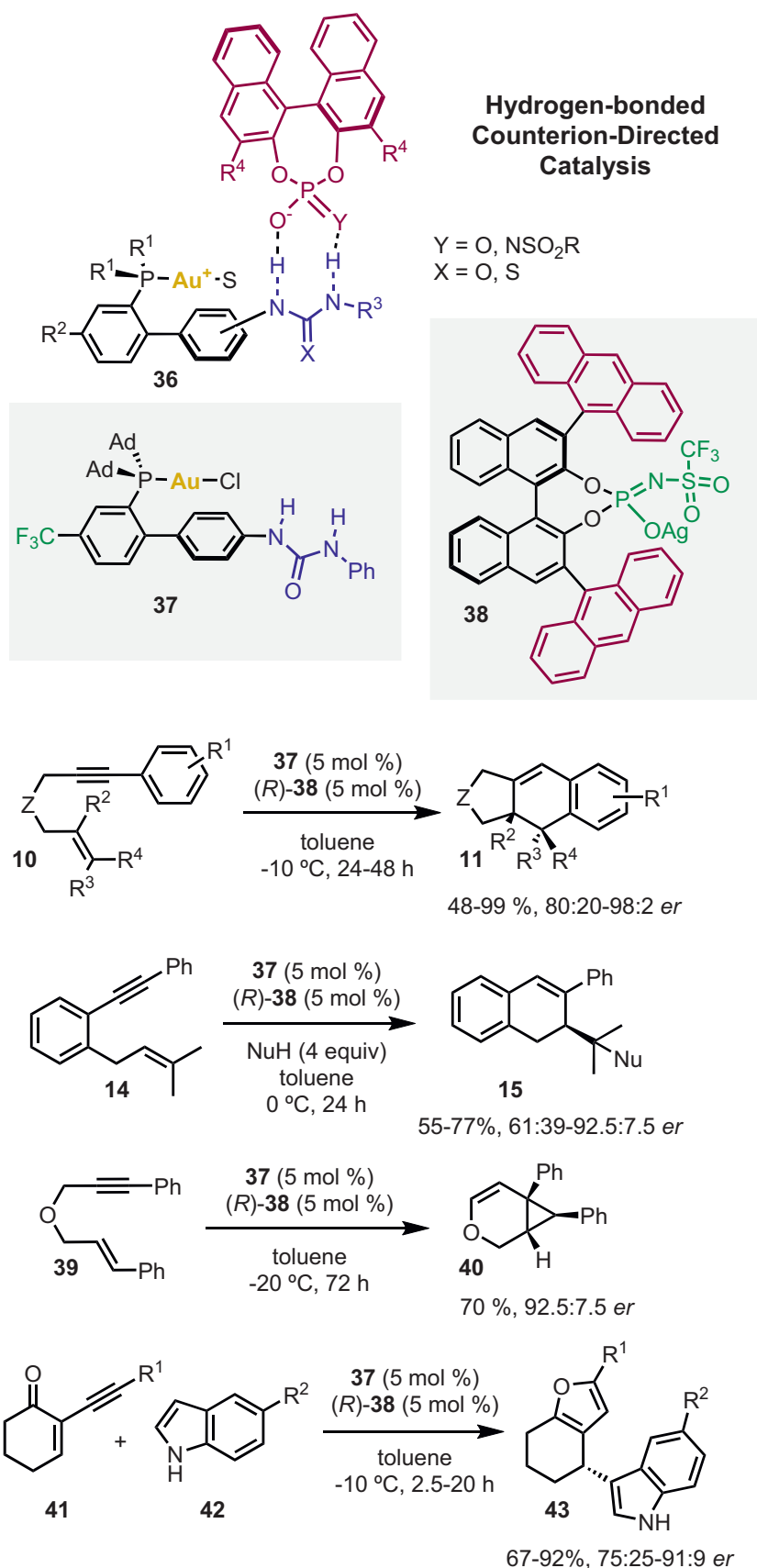
**Scheme 11** Chiral gold(I) resorcene[4]arene cavitand **31** and its applications in gold(I) catalysis and total synthesis.

be conducted on a 2-mmol scale using only 1 mol% of **37/38** (**Scheme 12**).

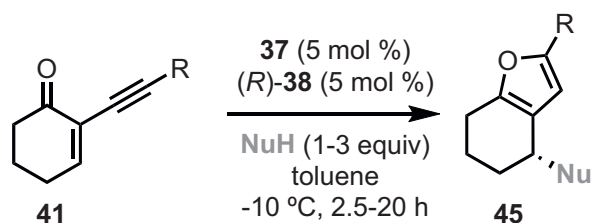
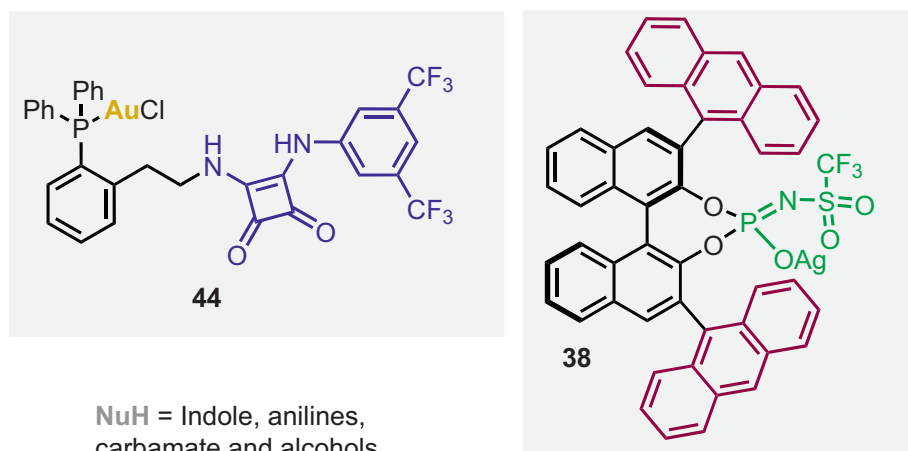
The enantioselective 6-*endo-dig* cyclization/nucleophilic addition of **14** and the cycloisomerization of **39** could also be performed in good yields and high enantioselectivities (**Scheme 12**). Similarly, the tandem cyclization of **41** and addition indoles **42** gave adducts **41** in moderate-to-good enantioselectivities.<sup>19</sup> Mechanistic investigations involving  $^1H$  NMR experiments, structure–activity studies of both components, and kinetic analysis supported the relevant role of H-bonding interactions and the

need of precise positioning of the chiral anion to achieve high enantioselectivity in this new approach. The breadth of the scope across different 1,6-enynes and consistent high enantiomeric ratios of this supramolecular chiral ligand system provide a new platform to develop challenging enantioselective metal-catalyzed transformations.

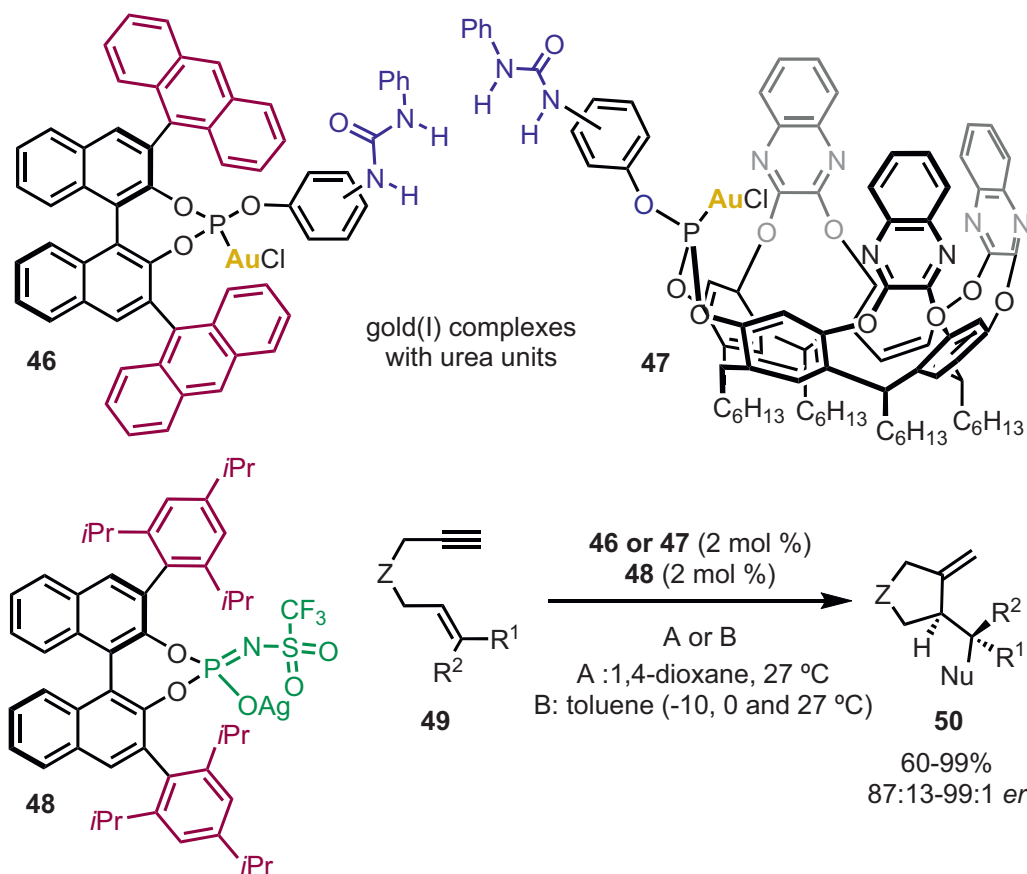
This approach was later expanded to the enantioselective gold(I) tandem cycloisomerization/nucleophile addition to 2-alkynyl enones **41** using H-bonded counterion-directed catalysis with a simpler gold(I) complex **44** bearing a squaramide



**Scheme 12** Concept of hydrogen-bonded counterion-directed enantioselective gold(I) catalysis **36** and achiral phosphinourea gold(I) complex **37**, chiral silver salt **38**, and applications of H-bonded asymmetric-counteranion directed catalysis (ACDC) in gold(I) catalysis.



**Scheme 13** Expansion of *H*-bonded counterion directed catalysis to tandem cyclization/nucleophile addition reaction.



**Scheme 14** Hydrogen-bonded matched ion pair gold(i) catalysis and enantioselective cyclization/nucleophile addition to 1,6-enynes.

(Scheme 13).<sup>20</sup> Other gold(I) complexes equipped with different H-donor donors were also studied. In comparison with the use of JohnPhos-type phosphino urea ligand, the scaffold of **44** presents higher flexibility to accommodate chiral anions. Initial studies gave bicyclic furans **45** in moderate yields when using the phosphino squaramide gold(I) complexes. High-throughput experimentation (HTE) was performed to evaluate combinations of seven chiral anions with seven achiral gold(I) complexes. The best results were obtained with a combination of **44** and (*R*)-**38** in toluene at low temperature. The scope of the tandem cycloisomerization/nucleophile addition was assessed using 1 mol% loading of **44**/*(R)*-**38**. Different variations on the indole, the enone substituents, as well as the use of diverse C-, N-, and O-based nucleophiles could be used to form corresponding tetrahydrobenzofurans **45** in excellent yields and enantiomeric ratios. Distinct modes of action were identified in the combinatorial screening, pointing at the versatility of H-bonded, counterion-directed catalysis to switch enantiofacial selectivity.

An evolution of the H-bonded ACDC concept combined chiral gold(I) complexes and chiral counterions, which allowed us to examine a match/mismatch situation.<sup>21</sup> A new library of gold(I) complexes inspired by chiral BINOL-based phosphites **2** (see Scheme 1) was prepared with diverse urea units at the *para*-, *meta*-, and *ortho*-positions with respect to the phenol fragment. In parallel, achiral phosphite cavitands with urea groups at the aryl of the phosphonite were prepared. Then, combinations of gold(I) complexes **46** and **47** with different chiral silver salts were tested using HTE in different cyclizations. The most promising results were obtained for the cyclization/nucleophile addition of 1,6-enynes **49** (Scheme 14). As expected, a match/mismatch scenario was observed when using the (*R*) and (*S*) enantiomers of the chiral silver salts. For the BINOL-based phosphite gold complexes, the best results were achieved with the match pair (*R*)-**46** and (*R*)-**48**, while in the case of phosphonite-based cavitands, **47** and (*R*)-**48** afforded the best results (Scheme 14). The scope of the tandem cycloisomerization/nucleophile addition was examined with (*R*)-**46** and (*R*)-**48** at 2 mol% in either 1,4-dioxane at 27 °C or toluene (−10, 0 and 27 °C). It is interesting to note that chiral silver salt (*R*)-**48** provided the best counterion for both phosphitoureia **46** and cavitand gold(I) **47** complexes.

Products **50** were consistently obtained with high levels of enantioselectivity across a broad set of 1,6-enynes and C-, N-, and O- nucleophiles, highlighting the robustness of this catalytic system.<sup>21</sup> NCI plots of the two possible transition states allowed the visualization of H-bond interactions between the H-bond donor and the phosphoramidate group, holding the two components together. Similarly, diverse attractive π–π stacking interactions between the aryl alkene of the substrate and the anthracenyl group of the chiral counterion were observed, which helped stabilizing the transition state. The catalytic system was also investigated in the formal [4+2] cycloaddition of 1,6-enynes **10** bearing internal alkynes and resulted in poor yields and moderate enantioselectivities. The small size of the chiral pocket generated by the ion pair may be behind the ineffectiveness of this approach with internal alkynes.

## 9 Concluding Remarks

The challenges imposed by the linear coordination that gold(I) complexes tend to adopt have given rise to creative ligand designs specifically tailored to achieve high enantioselectivity levels in reactions involving alkynes. Since our very first work on the enantioselective alkoxy cyclization with di-nuclear complexes,<sup>7</sup> our laboratory has introduced chiral gold(I) catalysts with novel ligands based on one-point binding P-ligands, phosphines, and phosphites in most cases, to which various chiral elements such as atropisomeric backbones, chiral 2,5-diaryl pyrrolidines, and chiral planar ferrocenes were introduced or used as templates. The variety of ligand scaffolds evolved from well-known BINOL-based phosphites and JohnPhos-type phosphines to unprecedented ferrocenyl ligands and bifunctional ligands. Likewise, our group has pioneered supramolecular approaches toward enantioselective gold(I) catalysis consisting of chiral phosphoramidites within resorcene[4]arene cavitands and H-bonded counterion-directed catalysis. This latter approach, in principle, seemed challenging because of the two-component nature of the systems and the delicate balance required among H-bonding, reactivity, and NCIs; however, it represents our most successful strategy toward enantioselective gold(I) catalysis. Lastly, the use of the recently introduced NEST analysis to evaluate the steric properties of linearly coordinated gold(I) complexes, along with well-established DFT methods, has greatly contributed to the design and development of novel electrophilic catalysts for the chiral folding of unsaturated substrates.

### Author affiliations

- 1 Institute of Chemical Research of Catalonia (ICIQ), Barcelona Institute of Science and Technology, Tarragona, Spain.
- 2 Departament de Química Orgànica i Analítica, Universitat Rovira i Virgili, C/ Marcel·lí Domingo s/n, Tarragona, Spain.

### Statements and additional information

**Conflict of Interest** The authors declare that they have no conflict of interest.

**Acknowledgment** We would like to thank all group members who contributed to the design of ligands and worked on their application in asymmetric gold(I) catalysis. We are also grateful to those who carried out early work on the discovery of new gold(I)-catalyzed cyclizations of 1,*n*-enynes for enlightening us of their mechanisms.

**Funding Information** We thank the MICIU (PID2022-136623NB-I00/MICIU/AEI/10.13039/501100011033/FEDER), UE and Severo Ochoa Excellence Accreditation CEX2024-001469-S funded by MCIU/AEI/10.13039/501100011033, the European Research Council (Advanced Grant 835080), the AGAUR (2021 SGR 01256), and the CERCA Program/Generalitat de Catalunya for financial support.

© 2025. The Author(s). This is an open access article published by Thieme under the terms of the Creative Commons Attribution-NonDerivative-NonCommercial-License, permitting copying and reproduction so long as the original work is given appropriate credit. Contents may not be used for commercial purposes, or adapted, remixed, transformed or built upon. (<https://creativecommons.org/licenses/by-nc-nd/4.0/>).

### References

- 1 (a) Fürstner A. *Chem Soc Rev* 2009; 38: 3208 (b) Shapiro ND, Toste FD. *Synlett* 2010: 675 (c) Obradors C, Echavarren AM. *Acc Chem Res* 2014; 47: 902 (d) Fensterbank L, Malacria M. *Acc Chem Res* 2014; 47: 953 (e) Dorel R, Echavarren AM. *Chem Rev* 2015; 115: 9028 (f) Pflästerer D, Hashmi ASK. *Chem*

- Soc Rev 2016; 45: 1331 (g) Echavarren AM, Muratore MN, López-Carrillo V, Escribano-Cuesta A, Huguet A, Obradors C. *Org React Vol.* 92; 2017; Chap 1
- 2 Teles JH, Brode S, Chabanas M. *Angew Chem Int Ed* 1998; 37: 1415
- 3 Mizushima E, Sato K, Hayashi T, Tanaka M. *Angew Chem Int Ed* 2002; 41: 4563
- 4 Hashmi ASK, Frost TM, Bats JW. *J Am Chem Soc* 2000; 122: 11553
- 5 (a) Muñoz MP, Adrio J, Carretero JC, Echavarren AM. *Organometallics* 2005; 24: 1293 (b) Khrakovsky DA, Tao C, Johnson MW, Thornbury RT, Shevick SL, Toste FD. *Angew Chem Int Ed* 2016; 55: 6079 (c) Johansson MJ, Gorin DJ, Staben ST, Toste FD. *J Am Chem Soc* 2005; 127: 18002 (d) Gawade SA, Bhunia S, Liu RS. *Angew Chem Int Ed* 2012; 51: 7835 (e) Solas M, Suárez-Pantiga S, Sanz R. *Angew Chem Int Ed* 2022; 61: e202207406 (f) Alonso I, Trillo B, López F et al. *J Am Chem Soc* 2009; 131: 13020 (g) Hamilton GL, Kang EJ, Mba M, Toste FD. *Science* 2007; 317: 496
- 6 Raducan M, Moreno M, Bour C, Echavarren MA. *Chem Commun* 2012; 48: 52
- 7 García-Morales C, Ranieri B, Escofet I et al. *J Am Chem Soc* 2017; 139: 13628
- 8 (a) Alcarazo M. *Chem Eur J* 2014; 20: 7868 (b) Cheng X, Zhang L. *CCS Chem* 1989; 2021: 3 (c) Zhang Z-M, Chen P, Li W, Niu Y, Zhao X-L, Zhang J. *Angew Chem Int Ed* 2014; 53: 4350 (d) Zhang P-C, Wang Y, Zhang Z-M, Zhang J. *Org Lett* 2018; 20: 7049 (e) Zhang Z, Smal V, Retailleau P et al. *J Am Chem Soc* 2020; 142: 3797 (f) Lin B, Xiao Y, Yang T, Chen GQ, Zhang XC. *C. iScience* 2024; 27: 110876 (g) Elías-Rodríguez P, Benítez M, Iglesias-Sigüenza J et al. *Org Lett* 2024; 26: 5995
- 9 Delpont N, Escofet I, Pérez-Galán P et al. *Catal Sci Technol* 2013; 3: 3007
- 10 Nieto-Oberhuber C, Pérez-Galán P, Herrero-Gómez E et al. *J Am Chem Soc* 2008; 130: 269
- 11 Zuccarello G, Mayans JG, Escofet I et al. *J Am Chem Soc* 2019; 141: 11858
- 12 Zuccarello G, Nannini LJ, Arroyo-Bondía A et al. *JACS Au* 2023; 3: 1742
- 13 Caniparoli U, Escofet I, Echavarren AM. *ACS Catal* 2022; 12: 3317
- 14 (a) Pizarro JD, Molina F, Fructos MR, Pérez PJ. *Organometallics* 2020; 39: 2553 (b) Ruch AA, Ellison MC, Nguyen JK et al. *Organometallics* 2021; 40: 1416
- 15 (a) Abbas Z, Hu X-H, Ali A, Xu Y-W, Hu X-P. *Tetrahedron Lett* 2020; 61: 151860 (b) Togni A, Burckhardt U, Gramlich V, Pregosin PS, Salzmann R. *J Am Chem Soc* 1996; 118: 1031
- 16 Mora P, Escofet I, Besora M, Cester Bonati F, Echavarren AM. *ACS Catal* 2025; 15: 2342
- 17 (a) Schramm MP, Kanaura M, Ito K, Ide M, Iwasawa T. *Eur J Org Chem* 2016: 813 (b) Endo N, Kanaura M, Schramm MP, Iwasawa T. *Eur J Org Chem* 2016: 2514 (c) Endo N, Inoue M, Iwasawa T. *Eur J Org Chem* 2018: 1136 (d) Ho TD, Schramm MP. *Eur J Org Chem* 2019: 5678 (e) Rusalí LE, Schramm MP. *Tetrahedron Lett* 2020; 61: 152333
- 18 Martín-Torres I, Ogalla G, Yang J-M, Rinaldi A, Echavarren AM. *Angew Chem Int Ed* 2021; 60: 9339
- 19 Franchino A, Martí À, Echavarren AM. *J Am Chem Soc* 2022; 144: 3497

20 Martí À, Montesinos-Magraner M, Echavarren AM, Franchino A. *Eur J Org Chem* 2022: e202200518

21 Martí À, Ogalla G, Echavarren AM. *ACS Catal* 2023; 13: 10217

## About the authors



### Pablo Mora

Pablo Mora was born in Yecla (Murcia, Spain). After a one-year stay as an Erasmus student at The Robert Gordon University (Aberdeen, UK) and one semester at the University of North Carolina at Greensboro (USA), he obtained his degree in Pharmacy at Universidad de Granada (Spain) in 2020. After 6 months as intern at Syngenta (Switzerland), he joined the research group of Prof. Echavarren at the Institute of Chemical Research of Catalonia (Tarragona, Spain) where he obtained his PhD (2025) working on the design of new chiral gold(I) complexes and their application in catalysis.



### Imma Escofet

Imma Escofet was born in La Granada, in the Alt Penedès region of Catalonia (Barcelona, Spain). She studied chemistry at the University of Barcelona (UB) and did her bachelor's thesis at the University of Aberdeen (Scotland, UK) under the supervision of Prof. Laurent Trembleau (2010). Then, she joined the research group of Prof. Antonio M. Echavarren at the Institute of Chemical Research of Catalonia (ICIQ) in Tarragona, as a laboratory engineer where she also completed her PhD studies (2020) working on computational mechanistic studies of gold(I) catalysis and design of new chiral ligands. In 2022, she was promoted as Scientific Group Coordinator in Prof. Echavarren's research group at ICIQ.



### Prof. Dr Antonio M. Echavarren

Prof. Dr Antonio M. Echavarren was born in Bilbao (Spain). He received his PhD at the Universidad Autónoma de Madrid (UAM, 1982). After a postdoctoral stay in Boston College and Colorado State University, he joined the Institute of Organic Chemistry of the CSIC in Madrid. In 1992, he returned to the UAM as a Professor of Organic Chemistry and, in 2004, he moved to Tarragona as a Group Leader at the Institute of Chemical Research of Catalonia (ICIQ). In 2013, he got an ERC adv. grant to develop gold catalysis and, in 2019, a second ERC adv. grant to develop new catalysts for the biomimetic cyclization of unsaturated substrates. He received the 2004 Janssen-Cytag Award in organic chemistry and the 2010 Medal of the Royal Spanish Chemical Society and an Arthur C. Cope Scholar Award from the ACS. He is the President of the Spanish Royal Society of Chemistry (RSEQ).